J Mater Sci: Mater Electron
DOI 10.1007/s10854-017-8090-0

Microwave dielectric properties of $Bi(Sc_{1/3}Mo_{2/3})O_4$ ceramics for LTCC applications

Zixing Wang[1] · Changlai Yuan[1,2] · Baohua Zhu[1] · Qin Feng[1,2] · Fei Liu[1] · Lei Miao[1] · Changrong Zhou[1,2] · Guohua Chen[1,2]

Received: 1 August 2017 / Accepted: 19 October 2017

Abstract A novel microwave dielectric ceramics $Bi(Sc_{1/3}Mo_{2/3})O_4$ with low firing temperature were prepared via the solid reaction method. The specimens have been characterized using scanning electron microscopy, X-ray diffraction, Raman spectroscopy and DC conductivity. The $Bi(Sc_{1/3}Mo_{2/3})O_4$ ceramics showed B-site ordered Scheelite-type structure with space group C2/c. Raman analysis indicated that prominent bands were attributed to the normal modes of vibration of MoO_4^{2-} tetrahedra. The dielectric loss of $Bi(Sc_{1/3}Mo_{2/3})O_4$ ceramics can be depended strongly the bulk conductivity by DC measurement. The superior microwave dielectric properties are achieved in the $Bi(Sc_{1/3}Mo_{2/3})O_4$ ceramic sintered at 875 °C/4 h, with dielectric constant ~ 25, $Q \times f$ ~ 51,716 GHz at 6.4522 GHz and temperature coefficient of resonance frequency ~ − 70.4 ppm/°C. It is a promising microwave dielectric material for low-temperature co-fired ceramics technology.

1 Introduction

Recently, microwave dielectric ceramics have been attracted much attention duo to the rapid advances in wireless communication, the Tactile Internet (5th generation wireless systems) and intelligent transport systems. In order to meet the requirement of higher integration, miniaturization and improved reliability, the low-temperature co-fired ceramic (LTCC) technology has been an important fabrication process for electronic devices [1–4]. Many dielectric materials with good microwave dielectric properties cannot be employed in LTCC technology duo to the high sintering temperature. The LTCC technology is required to have lower sintering temperature because melting point of the inner electrode material Ag is 961 °C. Thus, currently intensive search is going on to find various microwave dielectric ceramics with low firing temperatures less than 961 °C [5–8].

The compounds rich-Bi and Mo could be expected to possess low sintering temperature duo to low metal points of Bi_2O_3 (817 °C) and MoO_3 (795 °C). Recently, several literatures have reported the microwave dielectric properties of bismuth-based molybdates for LTCC applications [9, 10], as such the $Bi_2Mo_2O_9$ ceramic with ε_r ~ 38, $Q \times f$ ~ 12,500 GHz, τ_f ~ 31 ppm/°C and a low sintering temperature 620 °C [11]. In previous reports, the $Bi(Fe_{1/3}Mo_{2/3})O_4$ ceramics could be found to possess a monoclinic ordered scheelite structure, a low densification temperature at 830 °C and excellent microwave dielectric properties with ε_r ~ 27.2, $Q \times f$ ~ 14,500 GHz and τ_f ~ − 80 ppm/°C [12]. Moreover, the $Bi(Ga_{1/3}Mo_{2/3})O_4$ and $Bi(In_{1/3}Mo_{2/3})O_4$ ceramics could be also crystallized in a similar ordered scheelite structure [13, 14], while an analogous phase could not be formed in the situation of Al and Cr contained at the B site. Similar to $Bi(Fe_{1/3}Mo_{2/3})O_4$ ceramic, the superior microwave dielectric properties with ε_r ~ 25.2, $Q \times f$ ~ 40,000 GHz and τ_f ~ − 65 ppm/°C and ε_r ~ 26.1, $Q \times f$ ~ 49,800 GHz and τ_f ~ − 86 ppm/°C could be also achieved in $Bi(In_{1/3}Mo_{2/3})O_4$ and $Bi(Ga_{1/3}Mo_{2/3})O_4$ ceramics, respectively [13, 14]. Uwe Kolitsch et al. had demonstrated that the ordered scheelite structure was also found in $Bi(Sc_{1/3}Mo_{2/3})O_4$ ceramics [15]. However, up to now, the microwave dielectric properties of the $Bi(Sc_{1/3}Mo_{2/3})O_4$

✉ Changlai Yuan
Yclai-2002@163.com

[1] College of Material Science and Engineering, Guilin University of Electronic Technology, Guilin 541004, People's Republic of China

[2] Guangxi Key Laboratory of Information Materials, Guilin University of Electronic Technology, Guilin 541004, People's Republic of China

Published online: 26 October 2017

ceramics have not been reported. In present work, the phase evolutions, microstructures and microwave dielectric properties of the $Bi(Sc_{1/3}Mo_{2/3})O_4$ ceramics were studied in detail.

2 Experimental procedure

The $Bi(Sc_{1/3}Mo_{2/3})O_4$ microwave dielectric ceramics were prepared by the solid-state method. Appropriate amounts of pre-dried Bi_2O_3 (Aladdin, 99.9%), Sc_2O_3 (Aladdin, 99.9%), MoO_3 (Aladdin, 99.9%) were weighed according to the stoichiometric formulation of $Bi(Sc_{1/3}Mo_{2/3})O_4$. The mixed powders were ball milled for 24 h in alcohol using a polyethylene bottle and stabilized ZrO_2 milling media. Then, the mixed slurry were dried and calcined at 750 °C for 4 h. The calcined powders with 7 wt% of PVA, were pressed into disks with 11 mm in diameter and 5 mm at height under a pressure ~ 200 MPa, and then sintered at 825 ~ 900 °C in air for 4 h.

The crystal structure of $Bi(Sc_{1/3}Mo_{2/3})O_4$ ceramics were determined by X-ray diffraction (XRD) using a Bruker D8Advance system. The microstructural observation was performed by scanning electron microscopy (SEM: quanta 450 FEG, FEI). The microwave dielectric properties were measured by $TE_{01\delta}$ shielded cavity method [16] with a network analyzer (E5230C;Agilent,USA). Temperature coefficients of resonance frequency (τ_f) were determined with the following formula:

$$\tau_f = \frac{(f_{75} - f_{25}) \times 10^6}{50 \times f_{25}}$$

where f_{75} and f_{25} are the resonant frequencies at 75 and 25 °C, respectively. Raman spectroscopy analysis have been employed to achieve better understanding about the structure–property relationship of the $Bi(Sc_{1/3}Mo_{2/3})O_4$ ceramics.

For electrical characterization, the DC conductivity is employed to investigate the electrical properties of the $Bi(Sc_{1/3}Mo_{2/3})O_4$ ceramics in the temperature ranges 140–400 °C. Before the measurement, Ag paste was used as electrode and smeared on opposite pellet faces, dried, decomposed and hardened by gradually heating at 600 °C for 1 h. The value of the DC bulk conductivity has been calculated following the formula $\sigma_{dc} = t/R_bA$, where R_b is bulk resistance, t is thickness and A is area of the electrode deposited on the specimens.

3 Results and discussions

Figure 1 shows the XRD patterns of $Bi(Sc_{1/3}Mo_{2/3})O_4$ ceramics sintered at various temperatures. As shown in Fig. 1a, a single monoclinic scheelite structure with a space group C2/c (PDF: 40-0414) can be obtained at various sintering temperatures from 825 to 900 °C. The XRD results agreed well with those reported by references [15]. The crystal structure of $Bi(Sc_{1/3}Mo_{2/3})O_4$ has been reported to have Sc atoms in distorted octahedral co-ordination, while Fe^{III} atom in $Bi(Fe_{1/3}Mo_{2/3})O_4$ ceramic is tetrahedrally coordinated by O atoms [15]. In addition, as shown in the Fig. 1 b, with increasing sintering temperature from 825 to 900 °C, it is noted that the enlarged diffraction peak at 27.5° and 28.7° shifts firstly towards lower angle and then to higher angle. This implies that the crystal structure of $Bi(Sc_{1/3}Mo_{2/3})O_4$ ceramics with increasing sintering temperature is firstly expanded, and then compressed, resulting into a maximum cell volume at 875 °C. This could be related to the fact that more amount of Bi^{3+}, Sc^{3+} and Mo^{6+} ions diffused into crystal lattice with rise in sintering temperature because the

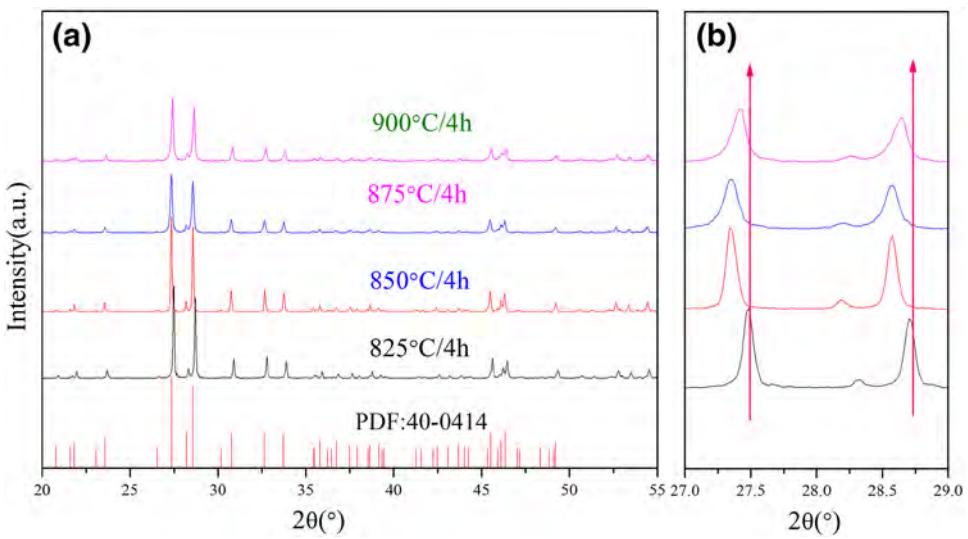

Fig. 1 X-ray diffraction patterns of $Bi(Sc_{1/3}Mo_{2/3})O_4$ ceramic sintered at the temperature of 825 ~ 900 °C

solubility increased with reasonable increasing of sintering temperature, leading to an increasement in cell volume at reasonable sintering temperature. The lattice parameters of $Bi(Sc_{1/3}Mo_{2/3})O_4$ prepared at 875 °C/4 h are $a = 16.60744$, $b = 11.55883$, $c = 5.21817$ and $\beta = 104.0128°$.

The room-temperature Raman spectra of $Bi(Sc_{1/3}Mo_{2/3})O_4$ ceramics in the frequency range 100–1000 cm^{-1} are shown in Fig. 2. According to the previous reports [17–20], the Raman fundamental modes for MoO_4 group are found to have four modes, namely, a mode v_1 at 894 cm^{-1} for non-degenerate symmetric stretching, a doubly degenerate symmetric bending mode v_2 at 407 cm^{-1}, the mode v_3 at 833 assigned to triply degenerate asymmetric stretching, and asymmetric bending v_4 modes at 381 cm^{-1}. Therefore, in this study, the mode at 865 cm^{-1} could be assigned to the $v_s(MoO_4)$ mode, while the modes at 317 and 344 cm^{-1} could be ascribed to the δ_s (MoO_4) mode and δ_{as} (MoO_4) mode, respectively. The extra band at 887 cm^{-1} is observed at the spectra, which might be associated with asymmetric stretching vibrations of MoO_4^{2-} ions. This can be the reason for that the distorted octahedral coordination of Sc in $Bi(Sc_{1/3}Mo_{2/3})O_4$ ceramics contrasts with the tetrahedral coordination of Fe in $Bi(Fe_{1/3}Mo_{2/3})O_4$. The Raman behavior of $Bi(Fe_{1/3}Mo_{2/3})O_4$ ceramics have been studied in detail [21], in which, the modes observed at 776 and 710 cm^{-1} could be assigned to δ_s (FeO_4) mode and δ_{as} (FeO_4) mode, respectively. Crystal structure of $Bi(Sc_{1/3}Mo_{2/3})O_4$ ceramics is similar to $Bi(Fe_{1/3}Mo_{2/3})O_4$, thus, the modes located at 775 and 712 cm^{-1} could be speculated to assign to δ_s (ScO_6) modes and δ_{as} (ScO_6) mode, respectively. Moreover, the Raman modes at 425 and 634 cm^{-1} could be detected in the $Bi(Fe_{1/3}Mo_{2/3})O_4$ ceramics. Similar Raman peak located at 437 and 613 cm^{-1} are also found in in the spectra

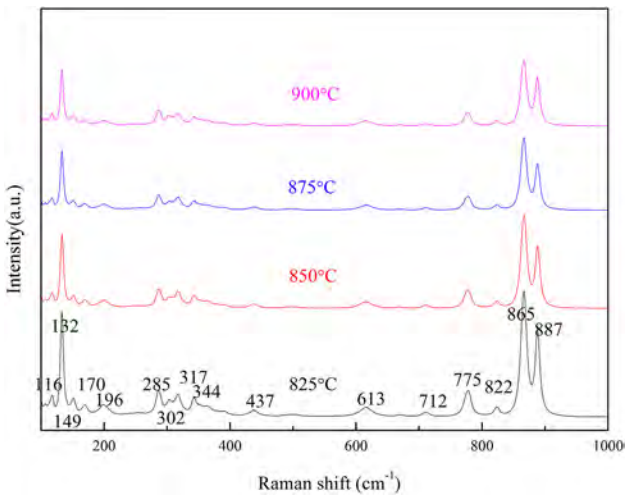

Fig. 2 The Raman scattering spectra of the $Bi(Sc_{1/3}Mo_{2/3})O_4$ ceramics after sintering at 825 ~ 900 °C

of $Bi(Sc_{1/3}Mo_{2/3})O_4$ ceramics, respectively. It is noted that a strong peak could be observed at 132 cm^{-1}, which might be assigned to the bending/wagging and external modes (such as Bi–O stretches), which is similar to other reports [22].The modes below 200 cm^{-1} should be assigned to the external modes (rotation/translation).

The SEM micrographs of $Bi(Sc_{1/3}Mo_{2/3})O_4$ ceramics sintered at different temperature are shown in Fig. 3. It is obvious that the porous microstructures could be developed from the SEM photos of the ceramics sintered at 825 °C and the grain size is smaller than 1 μm. As the temperature rises progressively, the pores could be gradually eliminated, and dense and homogenous microstructures with closely packed grains are obtained at optimum sintering temperature ~ 875 °C. Moreover, the grain sizes of the samples enlarge with the increasing sintering temperature. A further rise in the temperature to 900 °C leads to an oversintering, resulting in abnormal grain growth with larger grains in the samples. It is noted that the cylindrical grains could be formed for the samples sintered at 875 and 900 °C. In order to verify the compositions of $Bi(Sc_{1/3}Mo_{2/3})O_4$ ceramics, some grains of the samples sintered at 875 °C/4 h (as shown in Fig. 4) is analyzed by EDS. The EDS spectra in Fig. 4 indicated that the compositions were composed of elements Bi, Sc, Mo and O.

Figure 5 shows the variations in ε_r, $Q \times f$ values and τ_f of $Bi(Sc_{1/3}Mo_{2/3})O_4$ ceramics as a function of sintering temperature. As shown in Fig. 5a, the dielectric constant of $Bi(Sc_{1/3}Mo_{2/3})O_4$ ceramics increases firstly from 19.3 to 25 with the increasing sintering temperature from 825 to 875 °C, along with the elimination of pores during the sintering process. And the optimal $\varepsilon_r \sim 25$ could be achieved at the samples sintered at 875 °C. It is generally believed that the grain growth has a positive impact on the increasing of dielectric constant. However, when the sintering temperature further increased to 900 °C, the dielectric constant decrease slightly, which might be caused by the abnormal grain growth. This has been confirmed by SEM images, as shown in Fig. 3. Moreover, from the XRD analysis, there is an increase in cell volume with the increase of sintering temperature from the 825 to 875 °C. This could lead to an enlargement of the MoO_4^{2-} tetrahedron at B-site, subsequently, the increasement in amount of easier movement of Mo^{6+} ions in MoO_4^{2-} tetrahedron can raise the ionic electronic polarizability. Therefore, it is understandable that the maximum $\varepsilon_r \sim 25$ could be achieved for the sample sintered at 875 °C.

As shown in Fig. 5b, the effect of sintering temperature on $Q \times f$ values of the $Bi(Sc_{1/3}Mo_{2/3})O_4$ ceramics was demonstrated. When sintered at lower temperature ~ 825 °C, the specimens show a poor $Q \times f \sim 17{,}607$ GHz. With the increasing of sintering temperature, the $Q \times f$ value increased remarkably duo to grain growth and elimination

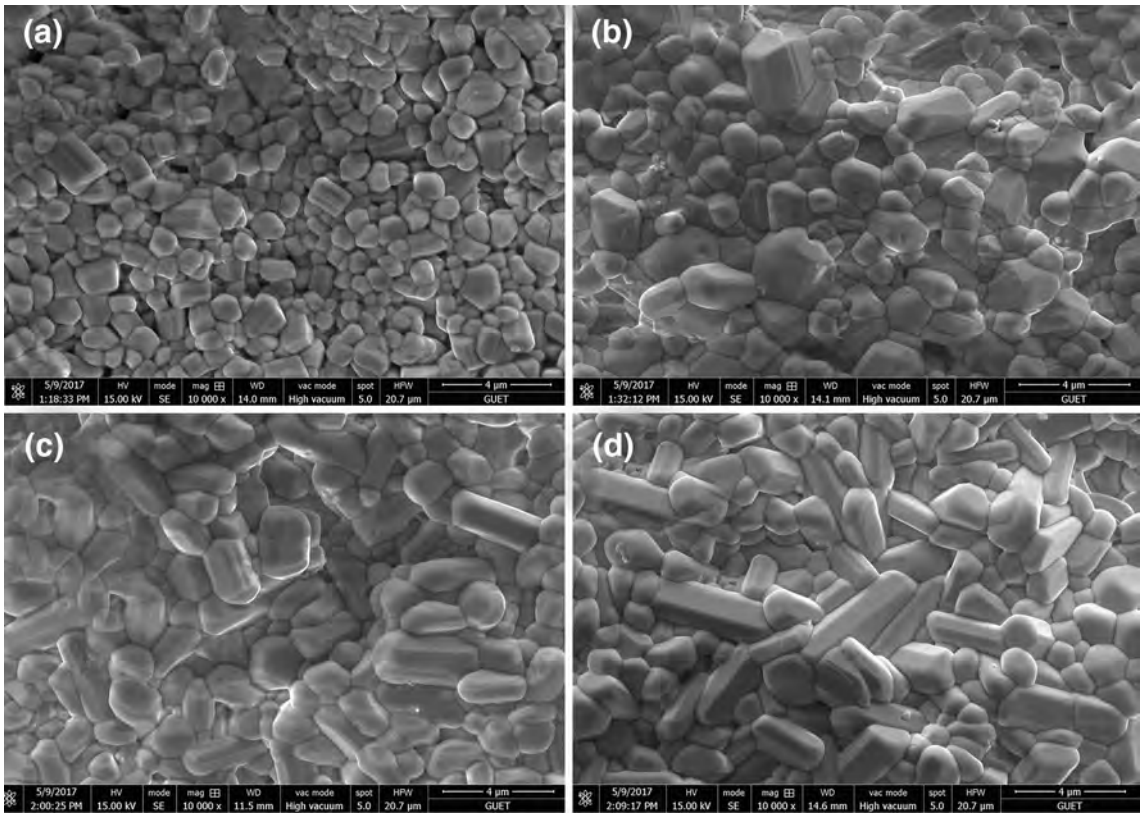

Fig. 3 SEM photos of $Bi(Sc_{1/3}Mo_{2/3})O_4$ ceramics sintered at **a** 825 °C/4 h, **b** 850 °C/4 h, **c** 875 °C/4 h and **d** 900 °C/4 h

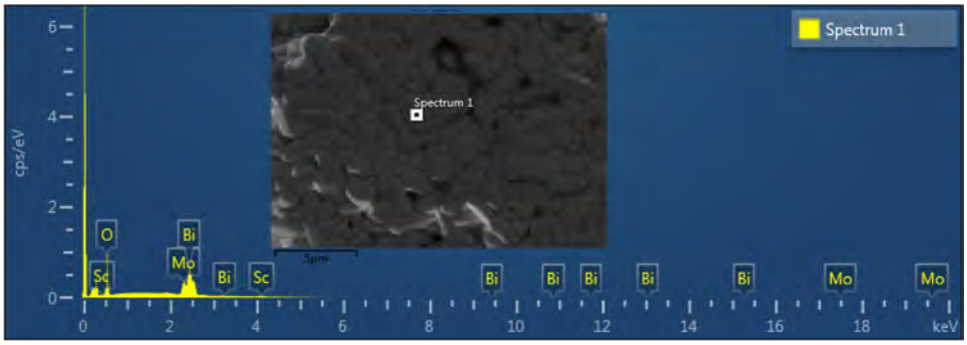

Fig. 4 EDS analysis of $Bi(Sc_{1/3}Mo_{2/3})O_4$ ceramic sintered at 875 °C/4 h

of pores. Up to 875 and 900 °C, the $Q \times f$ values increase to ~ 51,716 and 48,440 GHz, respectively. An optimal $Q \times f$ value ~ 51,716 GHz (at 6.4522 GHz) could be obtained after sintering at 875 °C for 4 h. Generally, microwave dielectric loss can be dominated by intrinsic loss and extrinsic loss. The extrinsic loss is associated with impurities, grain size, grain morphology and shape, secondary phase, pores, *etc* [23, 24]. The intrinsic dielectric loss is generally caused by absorptions of phonon oscillation [25]. The rises in average grain size and the decrease of pores are expected to obtain optimal $Q \times f$ value in dense ceramics. From the above SEM analysis, with increasing of the sintering temperature, no-obvious pores and proper grain size are found in the ceramics, which can help the achievement of good microwave dielectric properties. Therefore, here the $Q \times f$ values are mainly dominated by the extrinsic loss. The τ_f values of $Bi(Sc_{1/3}Mo_{2/3})O_4$ ceramics, as shown in Fig. 5c, are affected slightly by the sintering temperature. The τ_f values range from − 70.4 to − 85.5 ppm/°C for the specimens sintered at temperatures 825–900 °C.

The typical variation of DC conductivity of $Bi(Sc_{1/3}Mo_{2/3})O_4$ ceramics sintered different temperatures as a function of measured temperature is shown in Fig. 6. As shown in Fig. 6, the DC conductivity of the $Bi(Sc_{1/3}Mo_{2/3})O_4$ ceramics increased with rise in measured temperature, following Arrhenius behavior in the whole measured temperature

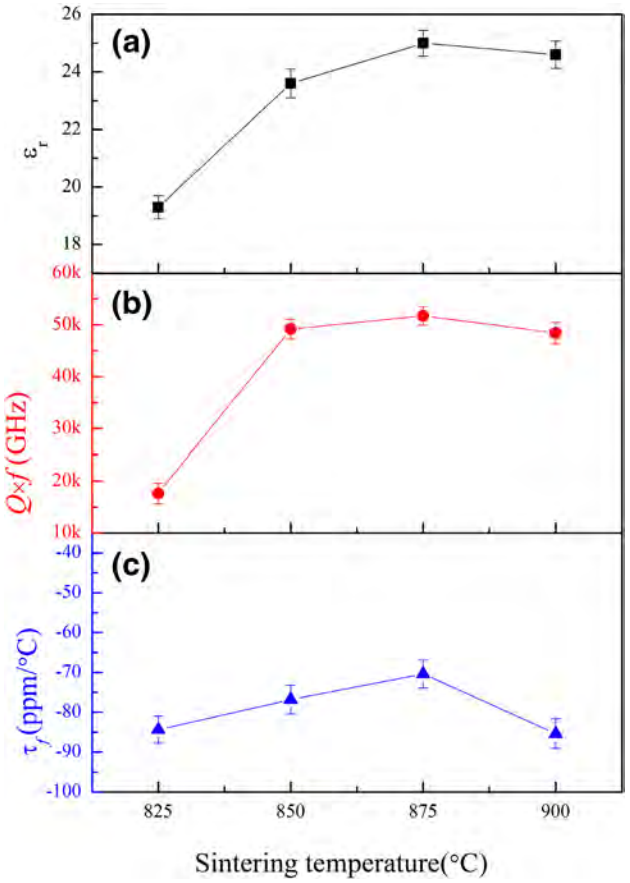

Fig. 5 The variations in ε_r, $Q\times f$ and τ_f of $Bi(Sc_{1/3}Mo_{2/3})O_4$ ceramics as a function of sintering temperature

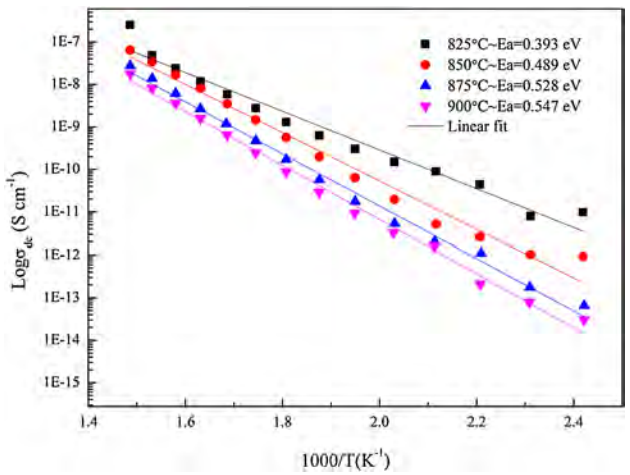

Fig. 6 Typical variation of DC conductivity of $Bi(Sc_{1/3}Mo_{2/3})O_4$ ceramics sintered different temperatures as a function of measured temperature at 140–400 °C

range. This suggests $Bi(Sc_{1/3}Mo_{2/3})O_4$ ceramics exhibited the negative temperature coefficient of resistance (NTCR) behavior. From the above SEM analysis, it is obvious that the $Bi(Sc_{1/3}Mo_{2/3})O_4$ ceramics sintered at higher temperature are more compact because of elimination of pores and grain growth. It implies that DC conductivity can be seriously affected by the pores among grains, namely, the more pores among grains, the higher conductivity. For dielectric materials, the bulk conductivity has a strong influence on the dielectric loss [26]. Therefore, it is understandable that the high $Q\times f$ values can be achieved at higher sintering temperature duo to the lower bulk conductivity. The activation energy (E_a) can be calculated by an empirical Arrhenius relation $\sigma=\sigma_0 \exp(-Ea/K_BT)$, where σ_0 is the pre-exponential factor and K_B is Boltzmann's constant, and T is the absolute temperature. With the rise in sintering temperature from 825 to 900 °C, the E_a values of the samples sintered at 825 and 900 °C are found to be 0.393, 0.547 eV, respectively. This suggests that the movement of oxygen vacancy existing in $Bi(Sc_{1/3}Mo_{2/3})O_4$ ceramics is very weak. An enhancement in crystallinity, a reduction in the number of defects in the grains/grain boundaries and grain growth are argued to lead to a high E_a [27].

4 Conclusion

In conclusion, phase pure $Bi(Sc_{1/3}Mo_{2/3})O_4$ ceramics has been synthesized by conventional solid-state route. The $Bi(Sc_{1/3}Mo_{2/3})O_4$ ceramics can be well densified below 900 °C. The XRD analysis indicates that the $Bi(Sc_{1/3}Mo_{2/3})O_4$ ceramics can be formed a B-site ordered Scheelite-type structure, with space group C2/c. The Raman spectroscopy analysis indicates that prominent bands are attributed to the normal modes of vibration of MoO_4^{2-} tetrahedra. The DC conductivity illustrates that the dielectric loss is depended strongly the bulk conductivity, namely, the higher $Q\times f$ values can result from the lower bulk conductivity. The ceramic sintered at 875 °C/4 h shows promising microwave dielectric properties, with $\varepsilon_r \sim 25$, $Q\times f \sim 51,716$ GHz (at 6.4522 GHz) and $\tau_f \sim -70.4$ ppm/°C. It is a promising microwave dielectric material for LTCC applications.

Acknowledgements Financial supports of the National Natural Science Foundation of China (Grants No. 11464006) and Guangxi Natural Science Foundation of China (Grant No. 2015GXNSFFA139002) are gratefully acknowledged by the authors.

References

1. A. Surjith, R. Ratheesh, High Q ceramics in the $ACe_2(MoO_4)_4$ (A = Ba, Sr and Ca) system for LTCC applications. J. Alloy. Compd. **550**, 169–172 (2013)

2. D. Zhou, H. Bin, J. Guo, L.X. Pang, Z.M. Qi, T. Shao, Q.P. Wang, Z.X. Yue, X. Yao, C. Randall, Phase evolution and microwave dielectric properties of $(Bi_{1-x}Fe_x)VO_4 (x < 0.40)$ ceramics. J. Am. Ceram. Soc. **97**, 2915–2920 (2014)
3. H.-H. Xi, D. Zhou, H.-D. Xie, W.-B. Li, Microwave dielectric properties of low firing $(Na_{0.5}Ln_{0.5})MoO_4$ (Ln=Nd and Ce) ceramics. Ceram. Int. **41**, 6103–6107 (2015)
4. J.J. Bian, Y.M. Ding, Structure, sintering behavior, and microwave dielectric properties of $(1–x)CaWO_4–xYLiF_4$ $(0.02 \le x \le 0.10)$ ceramics. Mater. Res. Bull. **67**, 245–250 (2015)
5. D. Zhou, C.A. Randall, L.-X. Pang, H. Wang, J. Guo, G.-Q. Zhang, X.-G. Wu, L. Shui, X. Yao, Microwave dielectric properties of Li_2WO_4 ceramic with ultra-low sintering temperature. J. Am. Ceram. Soc. **94**, 348–350 (2011)
6. D. Zhou, C.A. Randall, L.-X. Pang, H. Wang, X.-G. Wu, J. Guo, G.-Q. Zhang, L. Shui, X. Yao, Microwave dielectric properties of $Li_2(M^{2+})_2Mo_3O_{12}$ and $Li_3(M^{3+})Mo_3O_{12}$ (M=Zn, Ca, Al, and In) lyonsite-related-type ceramics with ultra-low sintering temperatures. J. Am. Ceram. Soc. **94**, 802–805 (2011)
7. J.J. Bian, L. Wang, Glass-free LTCC microwave ceramic-$(La_{0.5}Na_{0.5})_{1-x}(Li_{0.5}Nd_{0.5})_xWO_4$. J. Am. Ceram. Soc. **94**, 3188–3191 (2011)
8. M.T. Sebastian, H. Wang, H. Jantunen, Low temperature co-fired ceramics with ultra-low sintering temperature: a review. Curr. Opin. Solid State Mater. Sci. **20**, 151–170 (2016)
9. D. Zhou, C.A. Randall, H. Wang, L.-X. Pang, X. Yao, Microwave dielectric ceramics in Li_2O-Bi_2O_3-MoO_3 system with ultra-low sintering temperatures. J. Am. Ceram. Soc. **93**, 1096–1100 (2010)
10. D. Zhou, H. Wang, L.X. Pang, C.A. Randall, X. Yao, Bi_2O_3-MoO_3 binary system: an alternative ultralow sintering temperature microwave dielectric. J. Am. Ceram. Soc. **92**, 2242–2246 (2009)
11. D. Zhou, H. Wang, X. Yao, L.X. Pang, Microwave dielectric properties of low temperature firing $Bi_2Mo_2O_9$ ceramic. J. Am. Ceram. Soc. **91**, 3419–3422 (2008)
12. D. Zhou, L.-X. Pang, J. Guo, Y. Wu, G.-Q. Zhang, H. Wang, X. Yao, Sintering behavior and microwave dielectric properties of novel low temperature firing $bi_3femo_2o_{12}$ ceramic. J. Adv. Dielectr. **1**, 379–382 (2011)
13. L.X. Pang, D. Zhou, J. Guo, Z.M. Qi, T. Shao, Microwave dielectric properties of scheelite structured low temperature fired $Bi(In_{1/3}Mo_{2/3})O_4$ ceramic. Ceram. Int. **39**, 4719–4722 (2013)
14. L.X. Pang, W.G. Liu, D. Zhou, Z.X. Yue, Novel glass-free low-temperature fired microwave dielectric ceramics: $Bi(Ga_{1/3}Mo_{2/3})O_4$. Ceram. Int. **42**, 4574–4577 (2016)
15. U. Kolitsch, E. Tillmanns, $Bi_3ScMo_2O_{12}$: the difference from $Bi_3FeMo_2O_{12}$. Acta Crystallographica **59**, 43–46 (2003)
16. J. Krupka, Precise measurements of the complex permittivity of dielectric materials at microwave frequencies. Mater. Chem. Phys. **79**, 195–198 (2003)
17. F.D. Hardcastle, I.E. Wachs, Molecular structure of molybdenum oxide in bismuth molybdates by Raman spectroscopy. J. Phys. Chem **95**, 10763–10772 (1991)
18. N.K. James, R. Ratheesh, Microwave dielectric properties of low-temperature sinterable $BaCe_2(MoO_4)_4$ ceramics. J. Am. Ceram. Soc. **93**, 931–933 (2010)
19. A. Surjith, N.K. James, R. Ratheesh, Synthesis, structural and microwave dielectric properties of $Al_2W_{3-x}Mo_xO_{12}$ $(x = 0–3)$ ceramics. J. Alloy. Compd. **509**, 9992–9995 (2011)
20. J. Dhanya, A.V. Basiluddeen, R. Ratheesh, Synthesis of ultra low temperature sinterable $Na_2Zn_5(MoO_4)_6$ ceramics and the effect of microstructure on microwave dielectric properties. Scripta Mater. **132**, 1–4 (2017)
21. D. Zhou, L.X. Pang, J. Guo, Z.M. Qi, T. Shao, X. Yao, C.A. Randall, Phase evolution, phase transition, and microwave dielectric properties of scheelite structured $xBi(Fe_{1/3}Mo_{2/3})O_4–(1–x)BiVO_4$ $(0.0 \le x \le 1.0)$ low temperature firing ceramics. J. Mater. Chem. **22**, 21412–21419 (2012)
22. D. Zhou, W.B. Li, L.X. Pang, J. Guo, Z.M. Qi, T. Shao, X. Yao, C.A. Randall, Phase evolution and microwave dielectric properties of $xBi_{2/3}MoO_4$-$(1−x)BiVO_4$ $(0.0 \le x \le 1.0)$ low temperature firing ceramics. Dalton Trans. **43**, 7290–7297 (2014)
23. S.J. Penn, A.N. Mcn., T. Alan, X. Wang, M. Xu, R. Michael, S. Kevin, Effect of porosity and grain size on the microwave dielectric properties of sintered alumina. J. Am. Ceram. Soc. **80**, 1885–1888 (1997)
24. L.F. Jie Lia, Hao Luo, Jibran Khaliq, Ying Tang, Chunchun Li, Li_4WO_5: a temperature stable low-firing microwave dielectric ceramic with rock salt structure. J. Eur. Ceram. Soc. **36**, 243–246 (2016)
25. E. Schlömann, Dielectric losses in ionic crystals with disordered charge distributions. Phys. Rev. **135**, A413-A419 (1964)
26. K. Chen, M. Huang, Y. Shen, Y. Lin, C.W. Nan, Enhancing ionic conductivity of $Li_{0.35}La_{0.55}TiO_3$ ceramics by introducing $Li_7La_3Zr_2O_{12}$. Electrochim. Acta **80**, 133–139 (2012)
27. J. Jose, M.A. Khadar, Role of grain boundaries on the electrical conductivity of nanophase zinc oxide. Mater. Sci. Eng. A **304–306**, 810–813 (2001)